

## Botulinum Toxins Inhibit the Antidiuretic Hormone (ADH)-Stimulated Increase in Rabbit Cortical Collecting-Tubule Water Permeability

R. Quigley<sup>1</sup>, P.Y. Chu<sup>2</sup>, C.L. Huang<sup>2</sup>

<sup>1</sup>Department of Pediatrics, University of Texas Southwestern Medical Center at Dallas, 5323 Harry Hines Blvd., Dallas, Texas 75235-9063, USA

<sup>2</sup>Department of Internal Medicine, University of Texas Southwestern Medical Center at Dallas, Dallas, Texas 75235-9063, USA

Received: 10 January 2005/Revised: 3 June 2005

**Abstract.** The mammalian renal collecting duct increases its water permeability in response to antidiuretic hormone (ADH). ADH causes cytoplasmic endosomes containing the water channel, aquaporin 2 (AQP2), to fuse with the apical membrane so that the water permeability of the tubule increases many times above baseline. SNARE proteins are involved in the docking and fusion of vesicles with the cell membrane in neuron synapses. Whether these proteins are involved in the fusion of vesicles to the cell membrane in other tissues is not entirely clear. In the present study, we examined the role of SNARE proteins in the insertion of water channels in the collecting-duct response to ADH by using botulinum toxins A, B and C. Toxins isolated from *Clostridium botulinum* are specific proteases that cleave different SNARE proteins and inactivate them. Tubules were perfused in vitro with botulinum toxin in the perfusate (50 nM for A and B and 15 nM for C). ADH (200 pM) was then added to the bath after baseline measurements of osmotic water permeability ( $P_f$ ) and the change in  $P_f$  was followed for one hour. Botulinum toxins significantly inhibited the maximum  $P_f$  by approximately 50%. Botulinum toxins A and C also decreased the rate of rise of  $P_f$ . Thus, SNARE proteins are involved in the insertion of the water channels in the collecting duct.

**Key words:** In vitro microperfusion — Osmotic water permeability — SNARE proteins

### Introduction

The mammalian collecting duct regulates its water permeability in response to antidiuretic hormone (ADH) (Skorecki et al., 1992). When the animal is well hydrated, ADH is suppressed and the water permeability of the collecting duct is close to zero. When the animal becomes dehydrated and plasma osmolality increases significantly, the pituitary releases ADH, which then binds to its receptor (V2R) on the basolateral membrane of the collecting duct and activates adenylate cyclase through G protein activation (Knepper & Inoue, 1997). The increase in cAMP activates protein kinase A, which in turn phosphorylates target proteins (Katsura et al., 1997). One of the proteins that is phosphorylated is aquaporin 2 (AQP2), the water channel located in the collecting duct that is responsive to ADH (Fushimi et al., 1993; Nielsen & Agre, 1995). The phosphorylation of AQP2 appears to be necessary for its translocation from subapically located endosomes to the apical plasma membrane (Fushimi, Sasaki & Marumo, 1997; Katsura et al., 1997). The movement of AQP2-containing endosomes is regulated by ADH, is thought to be a constant process that involves endocytosis and exocytosis, and has been termed the “shuttle” hypothesis (Wade, Stetson & Lewis, 1981).

The molecular events controlling docking of vesicles and subsequent fusion between vesicles and target membranes are best known for fusion of synaptic vesicles (Sudhof, 1995). This process is highly regulated by proteins involved in the docking and fusion process (Hays et al., 1994). These are collectively termed “SNARE” (soluble NSF attachment protein receptor) proteins and are ubiquitously expressed (Sollner et al., 1993; Rothman, 1994). There are target SNAREs (t-SNAREs) located on the target

membrane and vesicle SNAREs (v-SNAREs). The t-SNAREs include syntaxin and SNAP-25, while the v-SNAREs include synaptotagmin and VAMP (vesicle associated membrane protein).

Whether SNARE proteins are involved in fusion of vesicles in every tissue, including AQP2-containing vesicles, is not entirely clear. Recently, various proteins in the SNARE pathway have been identified in the kidney (Franki et al., 1995a; Liebenhoff & Rosenthal, 1995). These have been further localized to the collecting duct, including VAMP-2 (Nielsen et al., 1995), syntaxin-4 (Mandon et al., 1997), synaptogamin VIII (Kishore et al., 1998), and SNAP-23 (Inoue et al., 1998). In addition, the SNARE protein, cellubrevin, has been colocalized to the vesicles that contain AQP2, suggesting that cellubrevin could be involved in the trafficking process (Franki et al., 1995b). While they have been localized to the collecting duct, there is no functional evidence for their involvement in the exocytosis of the AQP2-containing vesicles.

Botulinum toxins are proteases derived from *Clostridium botulinum*. Unlike synthetic toxins, these natural toxins are proteases that are very specific; they are known to cleave SNARE proteins exclusively (Montecucco & Schiavo, 1994; Pellizzari et al., 1999). Botulinum toxins A, C, and E cleave SNAP-25, one of the t-SNARES, at a different specific site for each toxin. VAMP, one of the v-SNARES, is cleaved at specific sites by botulinum toxins B, D, F and G and by tetanus toxin. Botulinum toxin C is the only toxin that cleaves syntaxin, one of the t-SNARES (Pellizzari et al., 1999). Thus, these are not nonspecific cellular toxins, but rather very specific inhibitors of exocytosis by interfering with the docking and fusion machinery of the cell (Pellizzari et al., 1999).

The purpose of the present study was to determine if SNARE proteins are involved in the insertion of AQP2-containing vesicles. To do this, we employed botulinum toxins A, B and C in the isolated perfused rabbit cortical collecting duct.

## Materials and Methods

### IN VITRO TUBULE PERfusion

Cortical collecting tubules from New Zealand White rabbits were perfused in vitro as previously described (Burg et al., 1966; Quigley & Baum, 1991). Briefly, cortical collecting tubules were dissected in cooled (4°C) modified Hank's solution containing in mm: 137 NaCl, 5 KCl, 0.8 MgSO<sub>4</sub>, 0.33 Na<sub>2</sub>HPO<sub>4</sub>, 0.44 KH<sub>2</sub>PO<sub>4</sub>, 1 MgCl<sub>2</sub>, 10 Tris-HCl, 0.25 CaCl<sub>2</sub>, 2 glutamine and 2 L-lactate. This solution was bubbled with 100% O<sub>2</sub> and had a pH of 7.4. Tubules were then transferred to a 1.2 ml thermostatically controlled (38°C) bathing chamber and perfused with concentric glass pipettes. The perfusion solution contained in mm: 30 NaCl, 25 NaHCO<sub>3</sub>, 2,3 Na<sub>2</sub>HPO<sub>4</sub>, 10 Na acetate, 1.8 CaCl<sub>2</sub>, 1 MgSO<sub>4</sub>, 5 KCl, 8.3 glucose and 5 alanine and had an osmolality of 150 mOsm/kg water. The bathing solu-

tion was designed to simulate plasma and contained in mm: 115 NaCl, 25 NaHCO<sub>3</sub>, 2.3 Na<sub>2</sub>HPO<sub>4</sub>, 10 Na acetate, 1.8 CaCl<sub>2</sub>, 1 MgSO<sub>4</sub>, 5 KCl, 8.3 glucose and 5 alanine and also 6 g/dl of albumin. The osmolality of the bathing solution was 300 mOsm/kg water. The perfusion and bathing solutions were bubbled with 95% O<sub>2</sub> and 5% CO<sub>2</sub> at 37°C and had a pH of 7.4. The osmolalities of the perfusion and bathing solutions were measured with a Wide Range Osmometer (Advanced Instruments, Model WDW, Norwood, MA) and adjusted to the desired osmolality by the addition of water or NaCl. The bathing solution was exchanged at a rate of 0.5 ml/min to keep the osmolality and pH constant.

Volume absorption ( $J_v$  in nl/min-mm) was measured as the difference between the perfusion and collection rates and normalized per mm of tubule length. The collection rate was determined by timed collections using a constant volume pipette. Exhaustively dialyzed [methoxy-<sup>3</sup>H] inulin (New England Nuclear) was added to the perfusate at a concentration of 50 µCi/ml so that the perfusion rate could be calculated. The tubule length (L) was measured using an eyepiece micrometer.

The osmotic water permeability was calculated from the following equation (Al-Zahid et al., 1977):

$$P_f = -\frac{\dot{V}_0 C_0}{A V_w} \left[ \frac{C_0 - C_L}{C_0 C_b C_L} + \frac{1}{(C_b)^2} \ln \frac{(C_L - C_b) C_0}{(C_0 - C_b) C_L} \right]$$

where  $\dot{V}_0$  is the perfusion rate,  $C_0$ ,  $C_b$ , and  $C_L$  represent the osmolality of the perfusate, bath and collected fluid respectively,  $A$  is the surface area calculated from the inner radius and  $V_w$  is the molar volume of water. The collected fluid osmolality was calculated from the relationship:

$$C_L = \dot{V}_0 C_0 / \dot{V}_L$$

where  $\dot{V}_0$ ,  $\dot{V}_L$ ,  $C_0$ , and  $C_L$  have the same meaning as above.

The transepithelial potential difference (PD) was measured by using the perfusion pipet as the bridge into the tubular lumen. The recording and reference calomel half-cells were connected to the perfusion and bathing solutions via agarose bridges containing 3.6 M KCl/0.9 M KNO<sub>3</sub>. This arrangement avoided direct contact between the solution bathing the tubule and the KCl/KNO<sub>3</sub> agarose bridge. The recording and reference calomel half-cells were then connected to the high- and low- impedance sides, respectively, of an electrometer (model 601; Keithley Instruments, Inc., Cleveland Ohio).

In preliminary experiments, we found that incubation of the tubules with the toxins present in the luminal fluid for 1 to 2 hours had no effect on the ADH-stimulated water permeability. We then found that incubation for 4 hours prior to the addition of ADH was sufficient for the toxins to enter the cells and inhibit the ADH effect. Thus, tubules were perfused for three and one half hours prior to six control measurements of  $J_v$ ,  $P_f$  and PD. The protocol for the experiments is illustrated in Fig. 1. ADH (200 pM) was then added to the bathing solution after 4 hours of incubation in both control and toxin-treated tubules. Measurements were then made for one hour after the addition of ADH. To compare the results of control tubules to botulinum toxin-treated tubules, the time response of the osmotic water permeability was fit empirically to an exponential curve using Sigma-Plot. This allowed for the most precise measurement of the maximal  $P_f$  obtained.

We also performed a set of experiments to test the stability of this preparation by measuring <sup>14</sup>C-sucrose permeability. Tubules were perfused with the same perfusate as above except for the addition of sodium chloride to make the osmolality 300 mOsm/kg water (isotonic with the bathing solution) and the addition of <sup>14</sup>C-sucrose. Sucrose permeability was then calculated using the same equation that we have previously reported for mannitol permeability in isolated perfused tubules (Quigley & Baum, 1994). There

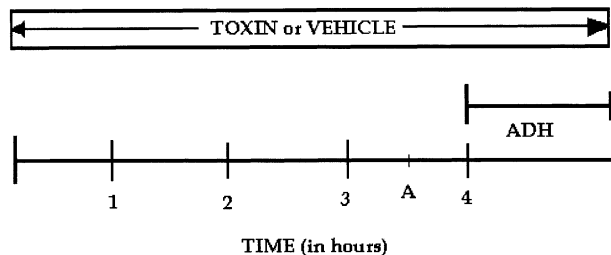


**Fig. 1.** Experimental protocol. Tubules were perfused with vehicle or toxin in the lumen for 3 and  $\frac{1}{2}$  hours. Then, control measurements of water permeability and potential difference were made beginning at time point A. ADH (200 pM) was then added to the bath and measurements continued for an additional hour.

was no difference between control tubules at 2 or 4 h ( $16.6 \pm 9.1$ , vs.  $13.6 \pm 7.9 \times 10^{-6}$  cm/s,  $n = 3$ ) or tubules perfused with toxin C for 2 or 4 h ( $12.9 \pm 6.3$ , vs.  $10.1 \pm 7.6 \times 10^{-6}$  cm/s,  $n = 3$ ). Thus, the tubule preparation appears to be very stable over this period of time and was not affected by toxin C.

In a separate set of experiments, tubules were perfused for 4 h in the presence of botulinum toxin A or vehicle. After the 4 h of perfusion, the tubules were fixed with 3% paraformaldehyde and 0.05% picric acid and allowed to fix while being perfused for another 20 min. The tubules were then transferred into 10% gelatin in PBS so that they could then be washed with PBS and embedded in OCT and sectioned as previously described by our laboratory (Chu et al., 2003). To perform *Clostridium botulinum* (Toxin-subtype A) / F-actin double immunofluorescence staining, the sections were preincubated for 3 h at room temperature with 8% milk powder in PBS containing 1% Triton X-100. They were then covered overnight at 4°C with the primary antibody, polyclonal rabbit antisera against *Clostridium botulinus* (Accurate Chemical & Scientific Corporation, Westbury, NY) at 1:50 dilution. The sections were rinsed four times with PBS prior to incubation for 80 min at room temperature with the secondary antibody, donkey anti-rabbit IgG conjugated to Rhodamine Red™-X (Jackson Immuno-Research Laboratories, West Grove, PA) at 1:100 dilution and with labeling F-actin, Alexa Fluor® 488 phalloidin (Molecular Probes, Inc., Eugene, OR) at 1:100 dilution, in the preincubation solution. After rinsing with PBS, the sections were mounted using VECTASHIELD® mounting medium (VECTOR Laboratories, Burlingame, CA). Fluorescent images were visualized through a Zeiss 40x or 100x objective lens using a laser scanning microscope (Zeiss LSM 410, Jena, Germany). To detect the fluorescence of Alexa Fluor, samples were excited at 495 nm and emissions were passed through a 518 band-pass filter. To detect fluorescence given by rhodamine, samples were excited at 568 nm and emissions were passed through a 590 band pass filter.

All data are expressed as mean  $\pm$  SEM. Comparisons between control and toxin-treated tubules were made by unpaired *t*-tests. Significance was determined by a *p* value less than 0.05.

## Results

### IMMUNOHISTOCHEMISTRY OF IN VITRO MICROPERFUSED CCD

Figure 2 shows the control and toxin A-treated tubules after 4 h of incubation. The control tubule (Panel A) shows no staining for the toxin A. Thus, the

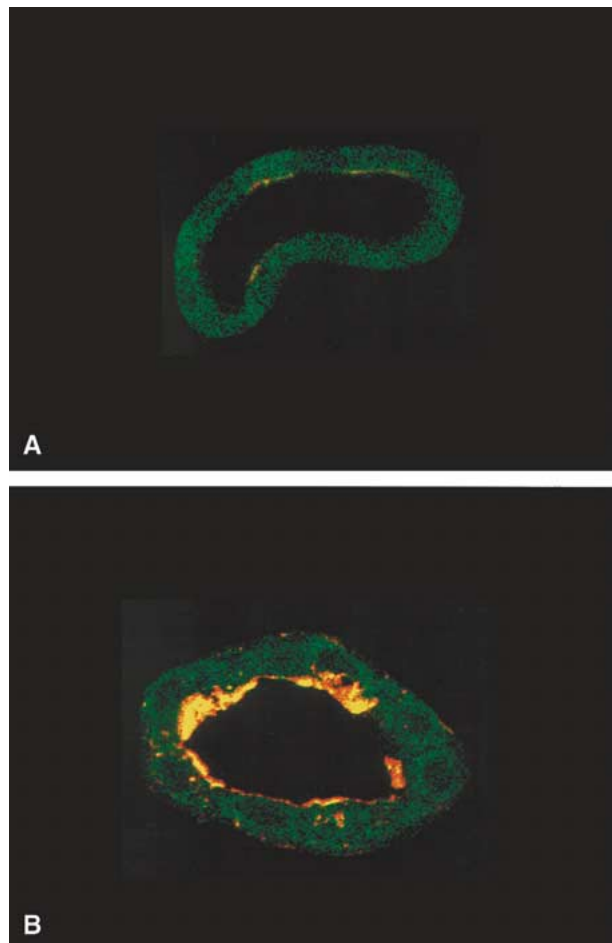


**Fig. 2.** (A) Control tubule after 4 hours of perfusion with vehicle. Tubule was perfused and fixed in vitro. Rhodamine red-conjugated phalloidin was used to label the actin cytoskeleton. Antibodies for botulinum toxin A were also used as the primary antibody. As can be seen, there was no staining for the toxin A. (B) Toxin A-treated tubule. The tubule was perfused and fixed in vitro. Botulinum toxin A was present in the lumen throughout this experiment. The luminal membrane and the subapical space stain heavily for toxin A. Thus, we believe that with time the toxin binds to the apical membrane and is endocytosed.

antibody used for the toxin A is not binding non-specifically to the tubule. In the toxin-treated tubule (shown in Panel B), toxin is seen intensely on the apical membrane and to some extent colocalizing with the actin. This indicates that toxin A can bind to the apical membrane and with time can be internalized. Also, the toxin-treated tubule shows no staining for the toxin when the primary antibody is absent (*not shown*).

### WATER PERMEABILITY RESPONSE TO ADH

Figure 3 shows the control response of the CCD  $P_f$  to ADH. The baseline water permeability in control tubules was low ( $36.2 \pm 11.9 \mu\text{m/s}$ ) and not affected by any of the toxins studied (see Table 1). Thus, the

**Table 1.** Effect of botulinum toxins on water permeability  $P_f$ 

	<i>N</i>	Baseline $P_f$ ( $\mu\text{m/s}$ )	Maximum $P_f$ ( $\mu\text{m/s}$ )
Control	9	36.2 $\pm$ 11.9	240.8 $\pm$ 13.2
Botox A	5	16.9 $\pm$ 8.5	98.7 $\pm$ 27.6*
Botox B	5	13.6 $\pm$ 16.9	158.4 $\pm$ 16.4*
Botox C	5	27.2 $\pm$ 8.6	129.3 $\pm$ 28.6*
A, B, and C	5	10.1 $\pm$ 3.4	79.7 $\pm$ 16.7*

\* $p < 0.05$  vs control

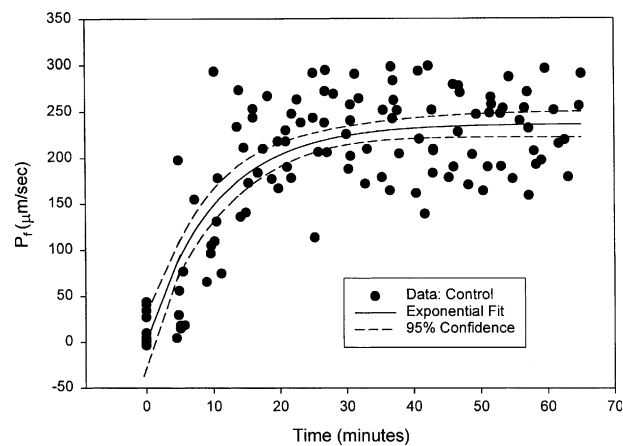
baseline properties of water transport in the CCD were not altered by treatment with the toxins, suggesting the absence of nonspecific effects of the toxins. After addition of ADH (200 pM), there was a prompt increase in the water permeability, which reached a plateau after 35–40 minutes. The data for each experiment were fit to an exponential curve to obtain the maximum  $P_f$  (see Table). For graphical comparison, the control data were also pooled together to obtain an overall exponential fit with a 95% confidence limit for the exponential fit that is also shown in Fig. 3.

Figure 4 shows the response of the CCD  $P_f$  to ADH after treatment with botulinum toxin A. This toxin cleaves SNAP-25, one of the t-SNAREs. As can be seen, the maximum  $P_f$  was about 50% of the control value (see Table 1). For comparison, also shown in Fig. 4 are the exponential fit and 95% confidence limit for the control experiments. As can be seen, there was no overlap between the fitted curve for the control experiments and that of the toxin A-treated tubules.

The response to ADH after treatment with botulinum toxin B is shown in Fig. 5. Botulinum toxin B, which specifically cleaves VAMP, reduced the maximum  $P_f$  response to ADH. Again, the maximum  $P_f$  is decreased from the maximum  $P_f$  of the control tubules. The exponential fit and 95% confidence limits for the control and toxin-treated tubules are also depicted.

Botulinum toxin C cleaves the t-SNARE, syntaxin. Fig. 6 shows the response of the CCD  $P_f$  to ADH after treatment with this toxin. As can be seen, the maximum  $P_f$  was about 50% of the control (see Table 1). The exponential fit and 95% confidence limits for the control and toxin-treated tubules are also shown.

The above series of studies demonstrated that the individual toxins that were tested did not completely block the effect of ADH on the CCD water permeability. The last series of experiments was performed to determine if a combination of toxins would be able to completely block the effect of ADH. These results are shown in Fig. 7 and in the Table. As can be seen, the combination of toxins A, B and C also inhibited the effect of ADH on the CCD water permeability response.



**Fig. 3.** Water-permeability response to ADH in control tubules. After three and  $\frac{1}{2}$  hours of perfusion, the tubules had a prompt response to ADH. Data were fit to an exponential curve for calculating the maximum response and the 95% confidence limits are shown.

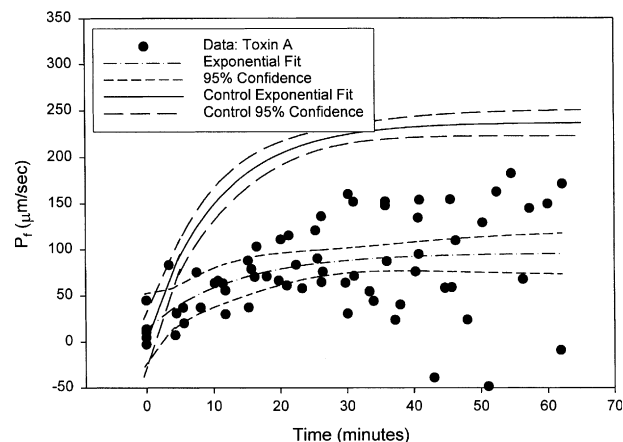


**Fig. 4.** Water permeability response in tubules treated with toxin A. Also depicted for comparison are the 95% confidence limits for the control tubules. As can be seen, botulinum toxin A had an inhibitory effect on the water permeability response.

Table 1 summarizes the data for the changes in water permeability in the CCD. The maximum  $P_f$  is significantly lower with each of the toxins as well as with the combination of all three toxins compared to control.

#### TRANSEPITHELIAL POTENTIAL DIFFERENCE

The lumen-negative transepithelial potential difference (*PD*) for control and toxin-treated tubules is shown in Fig. 8. As can be seen, the magnitude of the *PD* in the control tubules was significantly larger (i.e., more negative) than that for the tubules treated with toxins A and C, but was not different from tubules treated with toxin B. The *PD* in each tubule, however, was stable and did not decline with time, indi-

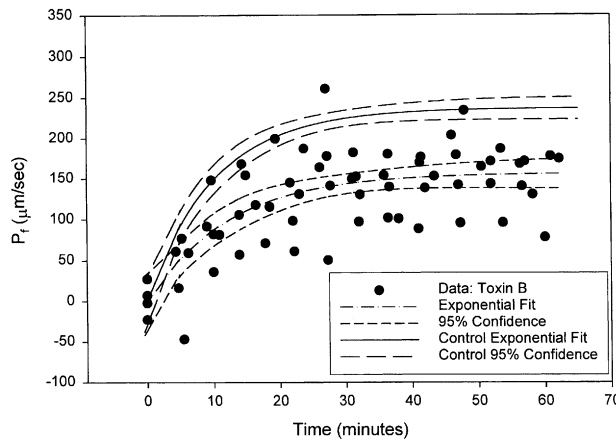


**Fig. 5.** Water-permeability response in tubules treated with toxin B. Also depicted for comparison are the 95% confidence limits for the control tubules. As can be seen, botulinum toxin B also had an inhibitory effect on the water permeability response.

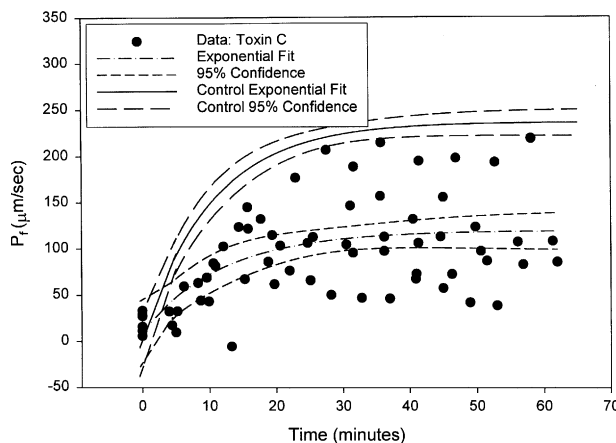


**Fig. 6.** Water-permeability response in tubules treated with toxin C. Also depicted for comparison are the 95% confidence limits for the control tubules. Botulinum toxin C also had an inhibitory effect on the water permeability response.

cating viability of the tubules throughout the experiment. All tubules had a transient increase in magnitude of the lumen-negative *PD* after treatment with ADH as previously described (Burg et al., 1968; Frindt & Burg, 1972). The *PD* went to zero after the addition of ouabain ( $10^{-5}$  M) to the bath at the end of the experiment (*data not shown*).

## Discussion

The current model for the acute regulation of the collecting duct water permeability response to ADH involves the shuttling of AQP2 water channels into and out of its apical membrane (Knepper & Inoue, 1997; Wade et al., 1981). The basolateral membrane contains other water channels (AQP3 and AQP4)

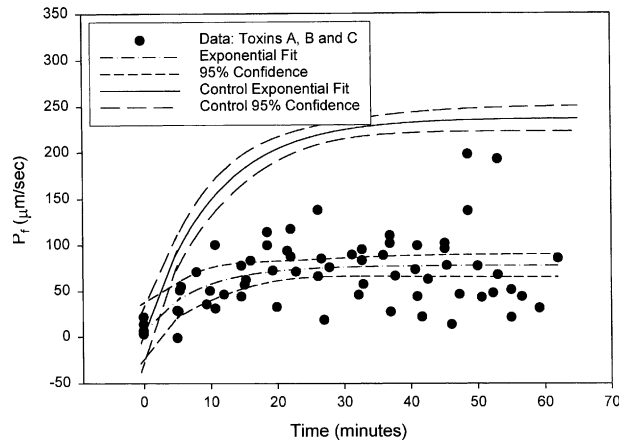


**Fig. 7.** Water-permeability response in tubules treated with toxins A, B and C. Also depicted for comparison are the 95% confidence limits for the control tubules. The combination of all three toxins had an inhibitory effect on the water permeability response. The effect was not additive.

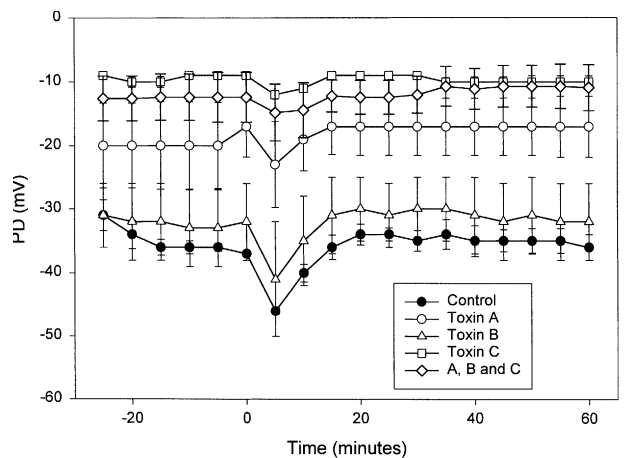


**Fig. 8.** Potential-difference response in tubules treated with vehicle or with botulinum toxins. Toxin B had no effect on the potential difference. However, toxin A and C and the combination had a significant effect on the potential difference.

that undergo long-term regulation, but have not been shown to participate in the acute regulation of water transport (Brown, Katsura & Gustafson, 1998). The process of insertion of the AQP2-containing vesicles into the apical membrane is thought to occur by the coordinated function of SNARE proteins (Hays et al., 1994; Knepper & Inoue, 1997). T-SNAREs residing in the apical membrane bind to v-SNAREs that reside in the vesicles to form a complex so that membrane fusion can occur. The t-SNARES that have been localized to the mammalian collecting duct are syntaxin-4 (Mandon et al., 1996) and SNAP-23 (Inoue et al., 1998). The primary v-SNARE that has been localized to the collecting duct is VAMP-2 (Nielsen et al., 1995). Another v-SNARE, synapto-

tagmin VIII, has also recently been found in the collecting duct (Kishore et al., 1998). The function of these proteins in the collecting duct is thought to be related to trafficking of transport proteins, primarily AQP2 (Knepper & Inoue, 1997). However, this has not been directly demonstrated.

The present study examined the role of these SNARE proteins in the ADH-stimulated increase in collecting-duct water permeability. In particular, the role of SNAP, VAMP and syntaxin were studied by employing botulinum toxins A, B and C, specific proteases for these proteins. The ability of the toxins to produce an effect depends on their ability to enter the cell and then cleave their target SNARE protein. Nerve cells have specific receptors for the toxins and are thus quite susceptible to their effects (Montecucco & Schiavo, 1994). The collecting duct principal cell has glycoproteins on its cell surface that may provide a binding site for the toxin. This is shown in Fig. 2 where there is intense staining of the tubule apical membrane for toxin A. The collecting duct cells have a continuous recycling of AQP2-containing vesicles that can then provide a pathway for the toxin to eventually enter the cell and cleave target SNARE proteins. We think that this explains the time dependence of the effect of the toxins seen in the present study.

We found that botulinum toxin A decreased the maximum  $P_f$  by about 50%. Toxin A cleaves SNAP-25 (Pellizzari et al., 1999). The homologue of SNAP-25 that has been found in the collecting duct is SNAP-23 (Inoue et al., 1998), which has been reported to be resistant to the action of botulinum toxin A (Chen et al., 1997). However, another group has reported that both SNAP-23 and SNAP-25 are in the collecting duct and has shown that botulinum toxin A inhibits the insertion of the  $H^+$  pump in the apical membrane of IMCD cells (Alexander, Shih & Schwartz, 1997; Banerjee et al. 1999). Thus, there appears to be functional SNAP-25 or an equivalent isoform in the collecting duct that is cleaved by toxin A.

We also found that botulinum toxin B lowers the maximum  $P_f$  of the rabbit cortical collecting duct. This toxin cleaves VAMP (Pellizzari et al., 1999). The isoform of VAMP that has been found in the collecting duct is VAMP-2 (Nielsen et al., 1995). This protein has also been found in other cell systems including rat parotid acinar cells, where the stimulated release of amylase from these cells was found to be inhibited by botulinum toxin B (Fujita-Yoshigaki et al., 1996). The authors had identified the presence of VAMP-2 in these cells and demonstrated that botulinum toxin B had no effect on baseline amylase secretion but inhibited the cAMP-stimulated secretion by about 50%. They also demonstrated that the amount of VAMP-2 that was cleaved in their preparation was also approximately 50%. In adipocytes, trafficking of GLUT-4-containing vesicles has also

been shown to be regulated by SNARE proteins, including the VAMP homologue, cellubrevin (Tellam et al., 1997). Recently, botulinum toxin B was shown to inhibit the insulin-stimulated increase in glucose uptake in 3T3-L1 adipocytes (Chen et al., 1997). The degree of inhibition was found to be between 30 and 60%, depending on the conditions studied. In rat IMCD cells in culture, VAMP was shown to be present and botulinum toxins A, B, C, D and tetanus toxin were shown to inhibit insertion of the proton pump (Alexander et al., 1997; Banerjee et al., 1999). The rate of pH recovery of these cells after treatment with the toxins was between 50 and 60% of the control cells. Thus, VAMP and its homologue are involved in multiple exocytosis pathways.

The role of syntaxin was examined using botulinum toxin C. This toxin reduced the maximum  $P_f$  by 50%. The syntaxin isoform in the collecting duct is syntaxin-4 (Mandon et al., 1996). Syntaxin-1 was originally thought to be confined to the nervous system but has now been found in epithelial cells (Naren et al., 2000). Its abundance in these tissues may be very low, but it may still be critical for the targeting of exocytic vesicles.

The inhibition of the ADH-stimulated water permeability in rabbit CCD in the present study was found to be 30–50%. The reason why the inhibition is not complete is not clear, but could be due to several factors. First, there is always a concern that since there are no specific receptors for the toxins on these cells (principal cells of the collecting duct), the amount of toxin entering the cell is minimal. In the nerve terminal, there are specific receptors for the toxins so that the amount of toxin that enters the cell is certainly much higher than that achieved in other tissues (Montecucco & Schiavo, 1994). To address this question, we used an antibody to botulinum toxin A to demonstrate that with time, the toxin binds to the apical membrane of the cortical collecting duct. We presume that the recycling of the apical membrane would then allow for entry of toxin that could then have its effect on the SNARE proteins. We think this explains the time dependency of this process.

Second, the stoichiometry of the SNARE proteins may be such that cleaving one of the proteins may only partially inhibit the process. We examined this possibility by perfusing the tubules with all three toxins. Thus, all possible targets of the botulinum toxins would be cleaved in the same tubule. Although there appeared to be a small difference with all the toxins, this was not statistically significant. Therefore, we do not think that the incomplete blockade of the ADH effect is due to differences in expression levels of the SNARE proteins.

Lastly, there may be a population of vesicles that are already docked and ready to fuse so that the toxin may only inhibit further recruitment of vesicles con-

taining AQP2 (Hays et al., 1994). We think that this is the most likely explanation of the incomplete effect of the toxins. It is interesting to compare our results to the above-mentioned studies that examine the effects of the toxins on non-neuronal tissue. All of these studies demonstrate that the toxins inhibit the insertion of endosomes by about 50%. Thus, we think that there may be a population of vesicles that are already docked and ready for fusion. The toxins then prevent the additional recruitment of vesicles to limit the maximum response.

The collecting duct also actively transports sodium and potassium. This is driven by the Na-K-ATPase that is located on the basolateral surface of the collecting-duct principal cells and maintains a low intracellular sodium concentration and a high potassium concentration. Sodium enters the cell from the tubule lumen via the epithelial sodium channel (ENaC) that produces the lumen-negative transepithelial potential difference in the rabbit collecting duct. Blocking ENaC with amiloride or dissipating the sodium gradient with the Na-K-ATPase inhibitor, ouabain, causes the transepithelial potential difference to go towards zero. Potassium is secreted by the principal cells by first entering through the basolateral Na-K-ATPase. The high intracellular potassium concentration favors exit through the apically located potassium channel, ROMK. This process causes the transepithelial potential to become more positive. Thus, the transepithelial potential is a balance between sodium reabsorption and potassium secretion.

In our study, we found that both toxins A and C reduced the magnitude of the lumen-negative PD. We demonstrated that toxin C had no effect on sucrose permeability over the four hours of incubation. Thus, we do not think that the change in the potential difference is due to nonspecific damage to the epithelium. The reduction of the magnitude of the negative PD may be due to an increase in potassium secretion through the ROMK channel or decrease in sodium reabsorption through ENaC. In addition to mediating vesicle fusion, there is increasing evidence that t-SNAREs such as syntaxin and SNAP-25 may also regulate the function of ion channels (Saxena, Quick & Warnock, 2000). Syntaxin and SNAP-25 have been shown to directly bind to the voltage-gated calcium channel and CFTR and inhibit the function of these channels (Rettig et al. 1996; Sheng, et al., 1994; Naren et al., 1997; Naren et al., 1998). Cleavage of syntaxin and SNAP by botulinum toxins C and A, respectively, releases the inhibition of these channels by syntaxin and SNAP-25. We have found that in *Xenopus* oocytes, expression of syntaxin binds ROMK and inhibits its activity (Huang et al., *unpublished data*). Thus it is possible that ROMK channels are also inhibited by direct binding to syntaxin and SNAP-25 in the rabbit collecting duct. Botulinum toxins C and

A release the inhibition of ROMK and cause an increase in the potassium secretion. The lack of effect of toxin B (which cleaves the v-SNARE, VAMP) on the PD is consistent with this possibility.

In the present study, we have demonstrated that botulinum toxins A, B and C inhibit the ADH-stimulated increase in the CCD water permeability. Because these toxins are specific proteases for the SNARE proteins, this demonstrates directly the involvement of SNARE proteins in the exocytosis of AQP2-containing vesicles. The effect of these toxins on the transepithelial potential difference also raises the possibility that t-SNAREs may be involved in the direct regulation of ion channels in this nephron segment.

This work was supported by National Institutes of Diabetes and Digestive and Kidney Diseases Grants DK54368 (C-L.H.). We thank Laurel Johnson for her able secretarial assistance and Sumana Chakravarty for her technical assistance.

## References

- Al-Zahid, G., Schafer, J.A., Troutman, S.L., Andreoli, T.E. 1977. Effect of antidiuretic hormone on water and solute permeation, and the activation energies for these processes, in mammalian cortical collecting tubules. *J. Membrane Biol.* **31**:103-129
- Alexander, E.A., Shih, T., Schwartz, J.H. 1997. H<sup>+</sup> secretion is inhibited by clostridial toxins in an inner medullary collecting duct cell line. *Am. J. Physiol.* **273**:F1054-F1057
- Banerjee, A., Shih, T., Alexander, E.A., Schwartz, J.H. 1999. SNARE proteins regulate H(+) -ATPase redistribution to the apical membrane in rat renal inner medullary collecting duct cells. *J. Biol. Chem.* **274**:26518-26522
- Brown, D., Katsura, T., Gustafson, C.E. 1998. Cellular mechanisms of aquaporin trafficking. *Am. J. Physiol.* **275**:F328-F331
- Burg, M., Grantham, J., Abramow, M., Orloff, J. 1966. Preparation and study of fragments of single rabbit nephrons. *Am. J. Physiol.* **210**:1293-1298
- Burg, M.B., Isaacson, L., Grantham, J., Orloff, J. 1968. Electrical properties of isolated perfused rabbit renal tubules. *Am. J. Physiol.* **215**:788-794
- Chen, F., Foran, P., Shone, C.C., Foster, K.A., Melling, J., Dolly, J.O. 1997. Botulinum neurotoxin B inhibits insulin-stimulated glucose uptake into 3T3-L1 adipocytes and cleaves cellubrevin unlike type A toxin which failed to proteolyze the SNAP-23 present. *Biochemistry* **36**:5719-5728
- Chu, P.Y., Quigley, R., Babich, V., Huang, C.L. 2003. Dietary potassium restriction stimulates endocytosis of ROMK channel in rat cortical collecting duct. *Am. J. Physiol.* **285**:F1179-F1187
- Franki, N., Macaluso, F., Gao, Y., Hays, R.M. 1995a. Vesicle fusion proteins in rat inner medullary collecting duct and amphibian bladder. *Am. J. Physiol.* **268**:C792-C797
- Franki, N., Macaluso, F., Schubert, W., Gunther, L., Hays, R.M. 1995b. Water channel-carrying vesicles in the rat IMCD contain cellubrevin. *Am. J. Physiol.* **269**:C797-C801
- Frindt, G., Burg, M.B. 1972. Effect of vasopressin on sodium transport in renal cortical collecting tubules. *Kidney Intern.* **1**:224-231
- Fujita-Yoshigaki, J., Dohke, Y., Hara-Yokoyama, M., Kamata, Y., Kozaki, S., Furuyama, S., Sugiya, H. 1996. Vesicle-asso-

ciated membrane protein 2 is essential for cAMP-regulated exocytosis in rat parotid acinar cells. The inhibition of cAMP-dependent amylase release by botulinum neurotoxin B. *J. Biol. Chem.* **271**:13130–13134

Fushimi, K., Sasaki, S., Marumo, F. 1997. Phosphorylation of serine 256 is required for cAMP-dependent regulatory exocytosis of the aquaporin-2 water channel. *J. Biol. Chem.* **272**:14800–14804

Fushimi, K., Uchida, S., Hara, Y., Hirata, Y., Marumo, F., Sasaki, S. 1993. Cloning and expression of apical membrane water channel of rat kidney collecting tubule. *Nature* **361**:549–552

Hays, R.M., Franki, N., Simon, H., Gao, Y. 1994. Antidiuretic hormone and exocytosis: lessons from neurosecretion. *Am. J. Physiol.* **267**:1507–1524

Inoue, T., Nielsen, S., Mandon, B., Terris, J., Kishore, B.K., Knepper, M.A. 1998. SNAP-23 in rat kidney: colocalization with aquaporin-2 in collecting duct vesicles. *Am. J. Physiol.* **275**:F752–760

Katsura, T., Gustafson, C.E., Ausiello, D.A., Brown, D. 1997. Protein kinase A phosphorylation is involved in regulated exocytosis of aquaporin-2 in transfected LLC-PK1 cells. *Am. J. Physiol.* **272**:F817–F822

Kishore, B.K., Wade, J.B., Schorr, K., Inoue, T., Mandon, B., Knepper, M.A. 1998. Expression of synaptotagmin VIII in rat kidney. *Am. J. Physiol.* **275**:F131–F142

Knepper, M.A., Inoue, T. 1997. Regulation of aquaporin-2 water channel trafficking by vasopressin. *Curr. Opin. Cell Biol.* **9**:560–564

Liebenhoff, U., Rosenthal, W. 1995. Identification of Rab3-, Rab5a- and synaptobrevin II-like proteins in a preparation of rat kidney vesicles containing the vasopressin-regulated water channel. *FEBS Lett.* **365**:209–213

Mandon, B., Chou, C.L., Nielsen, S., Knepper, M.A. 1996. Syntaxin-4 is localized to the apical plasma membrane of rat renal collecting duct cells: possible role in aquaporin-2 trafficking. *J. Clin. Invest.* **98**:906–913

Mandon, B., Nielsen, S., Kishore, B.K., Knepper, M.A. 1997. Expression of syntaxins in rat kidney. *Am. J. Physiol.* **273**:F718–F730

Montecucco, C., Schiavo, G. 1994. Mechanism of action of tetanus and botulinum neurotoxins. *Mol. Microbiol.* **13**:1–8

Naren, A.P., Di, A., Cormet-Boyaka, E., Boyaka, P.N., McGhee, J.R., Zhou, W., Akagawa, K., Fujiwara, T., Thome, U., Engelhardt, J.F., Nelson, D.J., Kirk, K.L. 2000. Syntaxin 1A is expressed in airway epithelial cells, where it modulates CFTR Cl<sup>-</sup> currents. *J. Clin. Invest.* **105**:377–386

Naren, A.P., Nelson, D.J., Xie, W., Jovov, B., Pevsner, J., Bennett, M.K., Benos, D.J., Quick, M.W., Kirk, K.L. 1997. Regulation of CFTR chloride channels by syntaxin and Munc18 isoforms. *Nature* **390**:302–305

Naren, A.P., Quick, M.W., Collawn, J.F., Nelson, D.J., Kirk, K.L. 1998. Syntaxin 1A inhibits CFTR chloride channels by means of domain-specific protein-protein interactions. *Proc. Natl. Acad. Sci. USA* **95**:10972–10977

Nielsen, S., Agre, P. 1995. The aquaporin family of water channels in kidney. *Kidney Intern.* **48**:1057–1068

Nielsen, S., Marples, D., Birn, H., Mohtashami, M., Dalby, N.O., Trimble, M., Knepper, M. 1995. Expression of VAMP-2-like protein in kidney collecting duct intracellular vesicles. Colocalization with Aquaporin-2 water channels. *J. Clin. Invest.* **96**:1834–1844

Pellizzari, R., Rossetto, O., Schiavo, G., Montecucco, C. 1999. Tetanus and botulinum neurotoxins: mechanism of action and therapeutic uses. *Phil. Trans. Roy. Soc. London* **354**:259–268

Quigley, R., Baum, M. 1991. Effects of growth hormone and insulin-like growth factor I on rabbit proximal convoluted tubule transport. *J. Clin. Invest.* **88**:368–374

Quigley, R., Baum, M. 1994. Effects of epidermal growth factor and transforming growth factor-alpha on rabbit proximal tubule solute transport. *Am. J. Physiol.* **266**:F459–F465

Rettig, J., Sheng, Z.H., Kim, D.K., Hodson, C.D., Snutch, T.P., Catterall, W.A. 1996. Isoform-specific interaction of the alpha1A subunits of brain Ca<sup>2+</sup> channels with the presynaptic proteins syntaxin and SNAP-25. *Proc. Natl. Acad. Sci. USA* **93**:7363–7368

Rothman, J.E. 1994. Mechanisms of intracellular protein transport. *Nature* **372**:55–63

Saxena, S., Quick, M.W., Warnock, D.G. 2000. Interaction of syntaxins with epithelial ion channels. *Curr. Opin. Nephrol. Hypertens.* **9**:523–527

Sheng, Z.H., Rettig, J., Takahashi, M., Catterall, W.A. 1994. Identification of a syntaxin-binding site on N-type calcium channels. *Neuron* **13**:1303–1313

Skorecki, K.L., Brown, D., Ercolani, L., Ausiello, D.A. 1992. Molecular mechanisms of vasopressin action in the kidney. In: *Handbook of Physiology, Chapter 26, Renal Physiology* pp 1185–1218 E.E. Windhager, ed. Oxford University Press

Sollner, T., Whiteheart, S.W., Brunner, M., Erdjument-Bromage, H., Geromanos, S., Tempst, P., Rothman, J.E. 1993. SNAP receptors implicated in vesicle targeting and fusion. *Nature* **362**:318–324

Sudhof, T.C. 1995. The synaptic vesicle cycle: a cascade of protein-protein interactions. *Nature* **375**:645–653

Tellam, J.T., Macaulay, S.L., McIntosh, S., Hewish, D.R., Ward, C.W., James, D.E. 1997. Characterization of Munc-18c and syntaxin-4 in 3T3-L1 adipocytes. Putative role in insulin-dependent movement of GLUT-4. *J. Biol. Chem.* **272**:6179–6186

Wade, J.B., Stetson, D.L., Lewis, S.A. 1981. ADH action: evidence for a membrane shuttle mechanism. *Ann. N. Y. Acad. Sci.* **372**:106–117